

# Meson Test Beam Momentum Selection

M. Backfish

February 18, 2016

## 1 Introduction

The purpose of this document is to describe mechanisms within the Meson Test beamline for momentum selection. This includes four simulations of the momentum spread or  $\frac{dP}{P}$  for the beam delivered to the experiments. The Meson Test, henceforward MTest, beamline layout can be seen in figure 1. Momentum selection in the MTest beamline is initially done with the Westward bending magnets MT4W-1 and MT4W-2. Initial momentum collimation occurs after these two dipoles with F:MT4CH1 and F:MT4CH2. These collimators can be fully extracted to around 90 mm or placed into the beamline with a gap of around 5 mm. MT5E, a five dipole string, bends the beam back East in order to better cancel dispersion from the first bend magnets. With collimators fully extracted the 76.2 mm aperture of MT5Q1 determines the momentum spread, or momentum bite, delivered to the experiments. In section 1 we use a simple geometric model to determine the momentum bite delivered without collimators. In section 2 we use a Turtle simulation to visualize the momentum selection based on a perfectly centered beam with no variations in horizontal or vertical positions, only variation in momentum spread [4]. In section 3 we vary the horizontal displacement and angle to determine the influence on the momentum spread. In section 4 we simulate an beam that is delivered into the secondary beamline off center horizontally to better understand the impact of upstream position variations from the target. The final sections of this paper describe the process used by operations to deliver the desired low momentum beams.

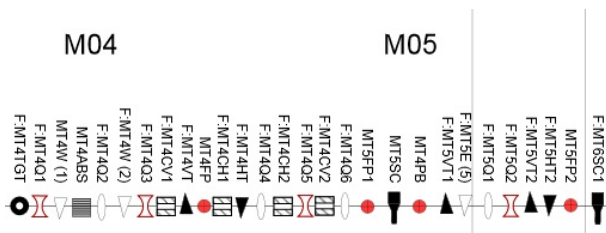


Figure 1: MTest secondary beamline components

## 2 Simplified Model for $2 \frac{GeV}{c}$ Beam

With momentum collimators fully extracted, 90 mm gap, the smallest momentum aperture becomes the first quadrupole after the MT5E bend string, MT5Q1. This is illustrated in figure 2.

To simplify the geometrical model, the total integrated field from all 5 magnets can be considered as one magnet as shown in figure 3. This is reasonable because the distance between the magnets is small in comparison to the length of the magnets. To account for some of the error caused by this assumption, the distance in between the magnets is then added to the final length of travel after the MT5E bend to the aperture at MT5Q1. Using the geometry outlined in figure 3 we find  $\frac{\Delta p}{p}$  to be  $\pm 4.5\%$ . This estimate is bigger than the actual as it neglects the momentum dependent position shift on the upstream end of MT5E as a result of MT4W (see figure 1 for beamline details).

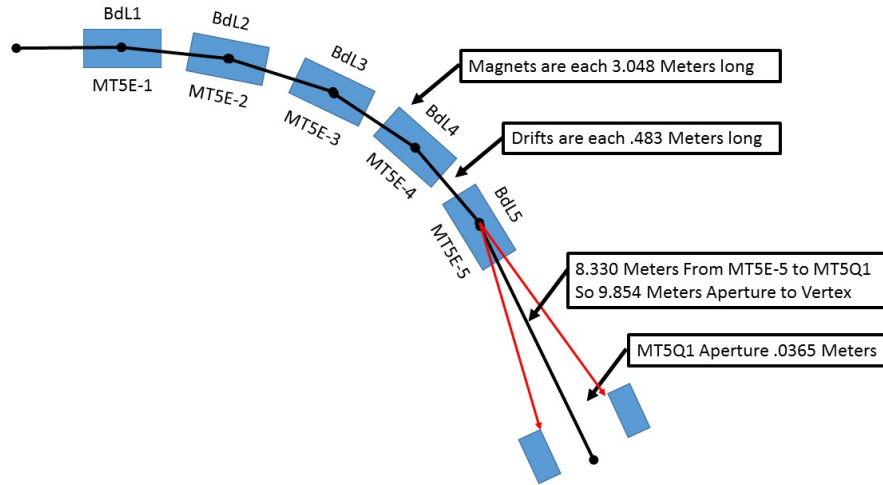


Figure 2: Off momentum particles will be bent more or less through the MT5E magnet string and ultimately deposited on the aperture of MT5Q1. It should be noted that each MT5E magnet bends the beam 8.5 mR or about .5 degrees. The angles are depicted larger in the image.

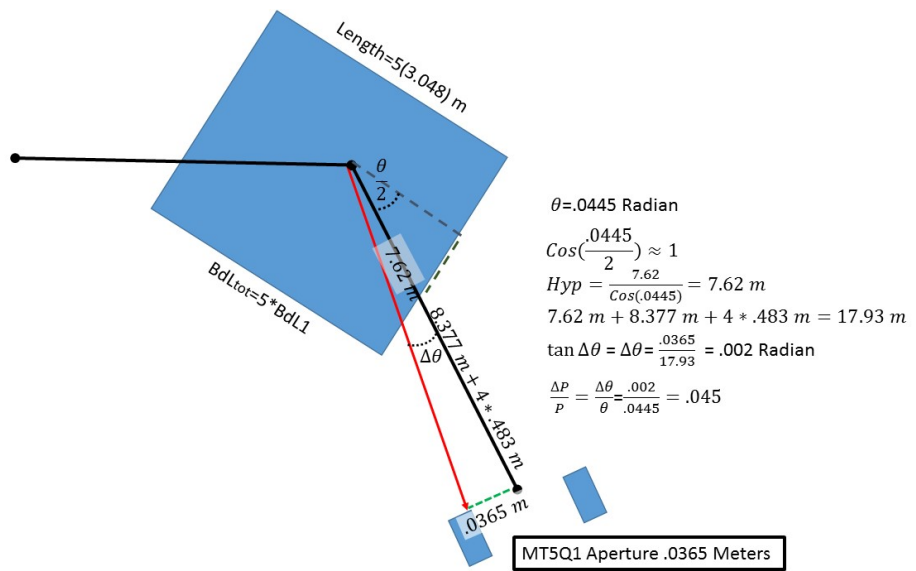


Figure 3: To simplify the model the total integrated field from all 5 magnets is considered as one magnet.

### 3 Simulation in Turtle with No Variations in Transverse Position or Angle

A detailed Transport/Turtle simulation was used to better understand how momentum selection occurs within the MTest beamline. Tracks were created with horizontal and vertical positions and angles equal to 0. Momentum spread,  $\frac{dP}{P}$ , was simulated from  $-10.000$  to  $10.000$  in  $.001$  increments. These vectors were propagated through the MTest beamline using Turtle and a  $2 \frac{GeV}{c}$  beam momentum. The results are displayed with a label of the component that caused the momentum restriction in figure 4. The simulations were performed with momentum collimators set to 90 mm or fully extracted from the beam. These results show that with MT4CH1 and MT4CH2 removed, the aperture of MT5Q1 determines the momentum bite. Figure 5 is a more detailed simulation which used initial particle vectors with  $\frac{dP}{P}$  from  $-1$  to  $.1$  in increments of  $.00001$ . The momentum spread is simulated downstream of the downstream cherenkov detector in MT6 Section 1. The momentum spread was found to be  $\pm 1.9\%$ .

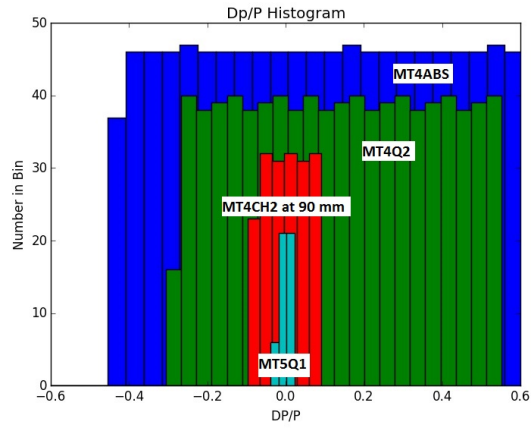


Figure 4: Momentum spread as simulated after each labeled device.

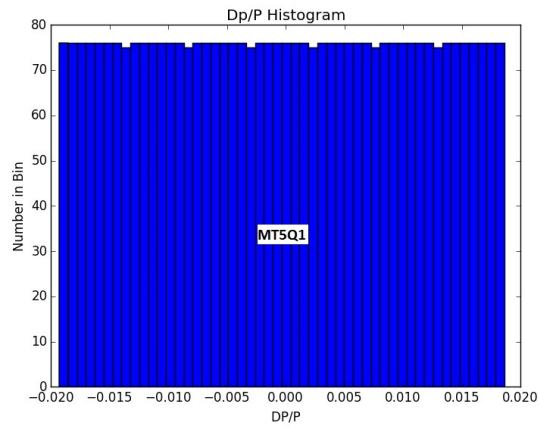


Figure 5: The first quad downstream of MT5Q1 ultimately determines the momentum spread at the experiment with upstream collimators fully extracted.

## 4 Simulation in Turtle Varying the Horizontal Positions and Angles

To better understand the impact of position and angle offsets into the secondary beamline,  $X$  is varied from  $-1$  mm to  $+1$  mm and  $X'$  from  $-1$  mR to  $+1$  mR. Momentum spread, or  $\frac{\Delta P}{P}$ , is varied from  $-0.10$  to  $+0.10$ . Histograms of these parameters are shown in figure 6. Momentums delivered to the downstream end of the second cherenkov (into MT6 section 1) are from  $-0.028$  to  $0.022$ . Using these extremities and momentum collimators at 90 mm (fully extracted), the momentum bite at the experiment is then  $0.025$  (2.5 %) with a  $-0.003$  (.3 %) offset favoring low momentum particles.

Using the same input vectors as shown in figure 6, the horizontal (momentum) collimators are then varied from 90 mm to 1 mm. There is little influence from the momentum collimators until they are set with less than a 20 mm gap. Figure 7 shows the momentums of the vectors transferred into MT6 section 1 with 20 mm, 10 mm, 5 mm, 3 mm, and 1 mm.

Thus far both MT4CH1 and MT4CH2 are set to the same value for each simulation. Figure 8 shows the momentums delivered into MT6 section 1 with both collimators at 5 mm along with a plot with the upstream collimator set to 90 mm. This plot suggests the downstream collimator is determining the momentum bite while the upstream collimator reduces intensities.

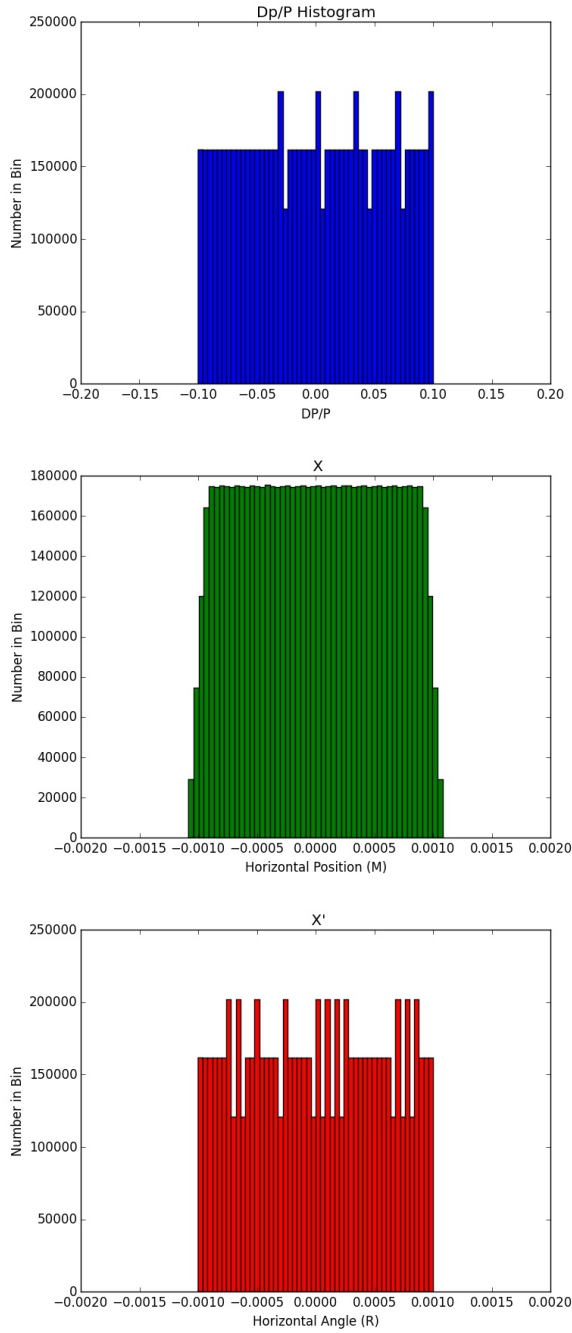


Figure 6: These histograms show the distribution of vectors that are initially fed into Turtle as tracks.

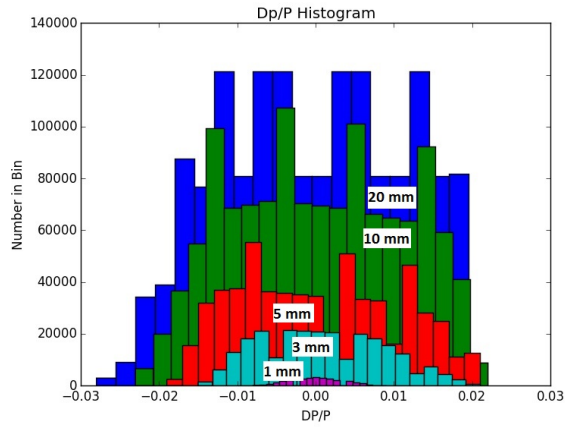


Figure 7: This histogram shows the momentum of the tracks that make it into the enclosure MT6 Section 1 with the momentum collimators set between 20 mm and 1 mm.

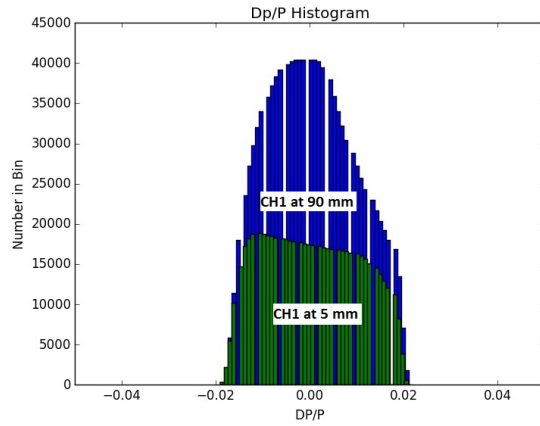


Figure 8: MT4CH2 determines the Momentum Bite in this simulation. If you remove MT4CH1, it does not change the momentum bite, but does impact the intensity of the beam delivered.

## 5 Simulation in Turtle Shifting the Horizontal Positions into the Beamline by $\pm 1.8$ mm

The MTest target shown in figure 9 is used to create the secondary beamline. Beam variations on target in April and May of 2015 are shown in figure 10. To better understand the impact of position variations going into the MTest secondary beamline, simulations were performed with both  $+1.8$  mm and  $-1.8$  mm horizontal position offsets as taken from the actual beam data. Momentum variations and position offsets for input tracks are shown in figure 11. Results of this simulation are shown in both figure 11 and table 1.

This simulations suggests a variation of  $\pm 1.8$  mm horizontally in the incoming beam can cause a  $\pm 3\%$  shift in the momentum of the beam delivered to the experiment while keeping the overall momentum bite the same. A more detailed simulation in MARS is needed to better understand the impact of position variations on target yield.

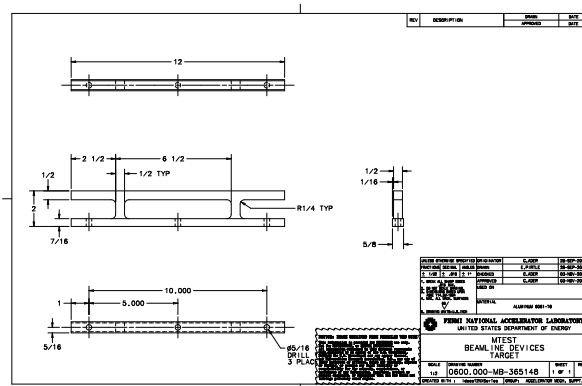


Figure 9: The MTest target is  $\frac{1}{2}$  in by  $\frac{1}{2}$  in by 12 in (12.7 mm by 12.7 mm by 304.8 mm) and made of Aluminum 6061-T6.

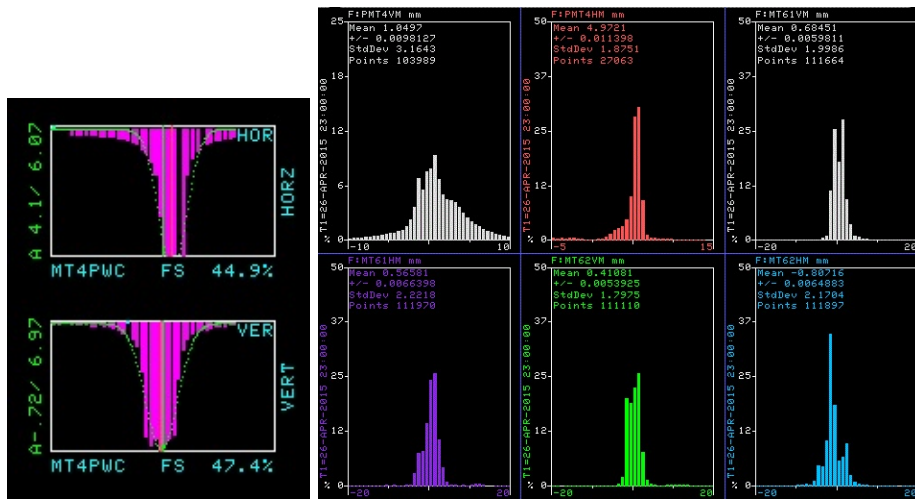


Figure 10: The left plot shows a characteristic wire profile for MT4PWC. The numbers to the left of each plot show the mean and width for each of the Gaussian fits also displayed. The right plot shows the distribution of the mean wire positions in MT4PWC From April 26, 2015 to May 26 2015. MT4PWC is just 0.425444 m before the target (MT4TGT). Note, these profiles are heavily dependent upon how the beam is tuned at the time. The quality of the fits vary from pulse to pulse.

Table 1: This table displays the results of varying the horizontal transverse position in which the beam enters the beamline. The values chosen are based on data position variations on target from April and May of 2015 as shown in figure 10. The average offset listed is the average of the minimum and maximum. Note there was initially an asymmetry in  $\frac{dP}{P}$  with a 0 mm offset in beam position input. Transport uses a right handed coordinate system thus when the beam shifts in the positive direction in transport the actual beam is moving West on target. Thus when the beam on target shifts  $-1.8$  mm or East, the momentum increases. As the beam on target moves West the momentum decreases.

Offset (mm)	Minimum	Maximum	$\frac{dP}{P}$	Avg. Offset
0.0	-.028	.022	2.5 %	-0.3 %
-1.8	-.024	.024	2.4 %	0.0 %
+1.8	-.031	.019	2.5 %	-0.6 %

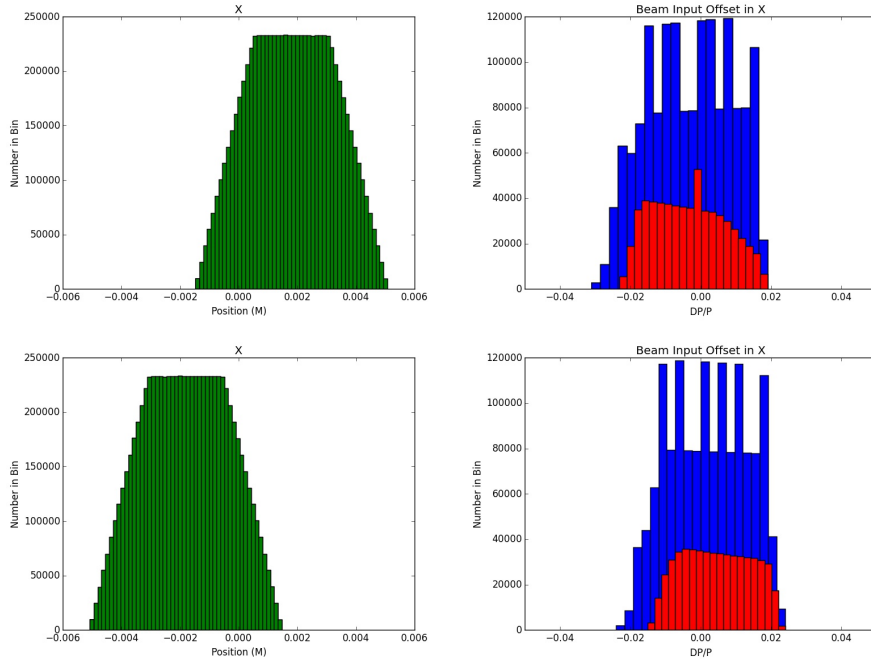


Figure 11: When the incoming beam is offset in the horizontal axis by 1.8 mm a small shift is seen in the central momentum though the momentum bite stays consistent. The left images show the variations in positions that were used as inputs into the simulations. The right images in blue show  $\frac{dP}{P}$  with both horizontal momentum collimators at 90 mm. The red histograms illustrate the same characteristics but with both collimators at 5 mm.

## 6 Conclusion

The rough geometrical calculation of momentum spread at the Fermi Test Beam Facility was  $\pm 4.5\%$  from section 1. This estimate should be larger than the actual momentum spread as upstream momentum dependent factors are assumed constant. The detailed simulation using Turtle with no transverse variations found  $\pm 1.9\%$  using a  $2 \frac{GeV}{c}$  beam. Varying transverse parameters increased the momentum spread to  $2.5\%$  and showed  $.3\%$  variations due to position offsets. More simulations need to be performed to understand how a transverse shift in target impact influences the particle yield off the target. The Fermi Test Beam Facility quotes  $\pm 2.7\%$  for the  $2 \frac{GeV}{c}$  beam momentum [3]. These simulations will be used and improved to better understand and control the Meson Test beam used at the Fermi Test Beam Facility.

## References

- [1] D.A. Edwards and M.J. Syphers, “An Introduction to the Physics of High Energy Accelerators”, Wiley Series in Beam Physics and Accelerator Technology, SSC laboratory, Dallas, Texas, 1993 pp. 61.
- [2] Eric Prebys, “Basic EM and Relativity”, USPAS, Austin, Tx 2012
- [3] A. Soha, <http://ppd.fnal.gov/ftbf/beam/energies.html>
- [4] D. Carey, Transport/Turtle Guide